Appl. Phys. B 39, 83–90 (1986)

Applied Physics B Photophysics and Laser Chemistry

Undamped Undulation Superposed on the Passive Q-Switching Pulse of a CO_2 Laser

M. Tachikawa, K. Tanii*, M. Kajita, and T. Shimizu

Department of Physics, University of Tokyo, Bunkyo-ku, Tokyo, 113 Japan

Received 23 August 1985/Accepted 19 October 1985

Abstract. An undamped undulation superposed on the pulse tail of the passive Q-switching is observed using HCOOH gas as a saturable absorber. The pulse shapes with the undulation are nicely reproduced through the rate-equation analysis in which the laser gain medium is described as a three-level system. Good agreements between the observation and the calculation are also obtained in the dependence of the period and the width of passive Q-switching pulse on laser parameters. The mechanism of the undulation is interpreted as the relaxation oscillation attributed to the relaxation from the lower laser level. The collisional rate constant of HCOOH molecule is also obtained.

PACS: 42.55, 42.65

A transient behavior in the gas laser oscillation has not been fully understood yet and there still remain several interesting problems to be solved. A detailed analysis of the process may also open a way to study dynamic properties of molecules.

A saturable absorber within the laser cavity causes repetitive spontaneous pulsation in the laser output. Since the passive Q-switching (P.Q.S.) in a CO_2 laser was first observed by Wood and Schwarz [1], the pulse shape and the repetition rate have been extensively studied by a number of authors using saturable absorbers such as CH_3Cl, CH_3F, SF_6, BCl_3, CH_3OH, and so on [2–17].

The P.Q.S. pulse was observed with a sharp spike followed by a tail which decayed exponentially until the laser stopped oscillating. Burak et al. reproduced the pulse shape by numerical integration of the rate equations based on the dual four-level model both in the laser medium and the absorber [9]. In the four-level system, both the initial and the final states of the infrared transition were independently coupled to a "rotational level bath" in each vibrational state.

Kreiner pointed out that the wiggles were observed before the cutoff of the P.Q.S. pulse [13]. Dupré et al. observed the pulse shape with two peaks at the beginning and ending parts of the P.Q.S. pulse and reproduced it through the numerical solution of the rate equations in the dual four-level model [11]. Šolajić and Heppner observed an oscillatory behaviour in the output of an ir–fir hybrid laser [18]. Recently Arimondo and Menchi reported that they found an undamped undulation nearly over the full tail of the P.Q.S. pulse with SF_6 [17]. However, the mechanism which causes the undulation was not fully understood.

We used HCOOH as a saturable absorber and observed the oscillatory behaviour on the tail of P.Q.S. pulse. In the present case, the undulation is much more prominent than those ever observed [13, 17, 18].

In this paper, we propose based on the results reported in [19, 20] that the undamped undulation on the P.Q.S. pulse is caused by the relaxation oscillation in the pulsed regime under the influence of the saturable absorber. Ueda and Shimizu (F.O.) reported that a relaxation oscillation was observed in the output of a 10.6 μm CO_2 laser in the afterglow region of the pulsed discharge [19]. This relaxation oscillation occurs in the competition between the rate of induced emission from the upper laser level and the rate of relaxation from the lower laser level. Shimoda observed the undamped relaxation oscillation in the output of the

* Permanent address: Chiyoda Institute of Technology, Taito-ku, Tokyo, 110 Japan

ruby laser and gave a successful theoretical explanation on this effect considering the saturation effects on the loss inside the gain medium [20].
We have employed the three-level · two-level model in which the laser gain medium and the absorbing gas are described as a three-level system and a two-level system, respectively, and succeeded in systematic reproduction of the pulse shape with the undulation for the first time.

1. Experimental Setup and Procedure

A schematic diagram of the experimental setup is shown in Fig. 1. The water-cooled laser discharge tube is 210 cm long and has a 15 mm inner diameter. The intra-cavity cell is 35 cm long. The length of the laser cavity is 350 cm. A concave mirror with a radius of 5 m and the grating (75 lines/mm) are located at the ends of the laser cavity. Two irises in the cavity make the laser oscillate on a TEM_{00} mode. The monochromator is employed to select a single laser line. The laser output is detected by a fast infrared detector (SAT A1), and the signal is introduced into a signal analyzer (IWATSU SM-2100A). The overall response time of the detecting system is 50 ns.
The laser gain tube is filled with a gas mixture of CO_2, N_2, and He (1 : 1 : 8). The total pressure in the gain tube is 8 Torr.
Among a number of frequency coincidences between the laser lines and the absorptive transitions of molecules, we found the favorable combination of the CO_2 laser 9 μm $R(20)$ line with the infrared transition v_6; $33_{0.33} \leftarrow 34_{0.34}$ of HCOOH for a study of the transient behavior of the laser oscillation. The absorption line is fairly strong and the frequency is 27 MHz higher than the laser frequency [21]. The transient oscillation is critically dependent on the laser parameters and a clear-cut undulation superposed on the P.Q.S. pulse is observed under feasible experimental conditions of the laser parameters.
In the experiment, the characteristics of P.Q.S. are investigated as functions of the discharge current in the gain tube and the partial pressure of He gas in the absorption cell (P_{He}). The He gas is added to vary the

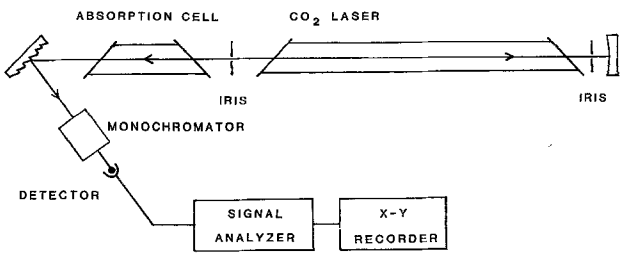

Fig. 1. Schematic diagram of experimental setup

relaxation rates of the relevant energy levels of HCOOH.

2. Experimental Results

The pulse shapes observed at several values of the discharge current are shown in Fig. 2a–d. The pressure of HCOOH is 77 mTorr. The pulse shows only the first spike when the discharge current is small. As the current is increased, the number of peaks of the undulation increases one by one, and the pulse tail becomes longer. When the current is increased further, the pulses in the P.Q.S. mode link each other, and then the laser oscillates in the cw mode. Figure 3 shows the period of the repeated P.Q.S. pulses as a function of the discharge current. The period has a minimum value, and this is consistent with the result of Arimondo and Menchi [17]. Figure 4 shows the change of the pulse width with the discharge current. The pulse width becomes larger monotonously with the increase of the current.
Figure 5a–e show the pulse shapes for several values of P_{He}, while the partial pressure of HCOOH is kept at 60 mTorr. The discharge current is 5 mA. The pulse width and then the number of peaks are critically dependent on P_{He}. Both decrease as P_{He} increases until the P.Q.S. pulse becomes a single spike at around $P_{He} = 300$ mTorr. As shown in Fig. 6, the pulse period also drastically decreases with the increase of P_{He} up to 100 mTorr, but remains almost constant at more than 300 mTorr.
As clearly seen in Figs. 2d or 5a, the amplitude of the undulation on the pulse tail decays in the beginning part of the pulse tail, remains almost constant (undamped undulation region), and then grows at the end of the pulse tail. The period of the undulation (the time interval between successive peaks) changes in a single pulse. The period in the ending part of the pulse (~24 μs) is about three times longer than that in the beginning part of the pulse (~8 μs). However the undulation period does not depend so much (up to 150%) on the discharge current and the He partial pressure.
The physical interpretation of the characteristic dependence of the pulse width and the pulse period on the discharge current and the partial pressure of He shown in Figs. 3, 4, and 6 can be given as follows. The rate of time variation in the gain (the population inversion in the laser medium) is determined by the difference between the induced emission rate and the pumping rate, and that in the loss (the sum of the cavity loss and the absorption loss by molecules) by the difference between the absorption rate and the relaxation rate. The laser starts oscillating when the gain overcomes the loss by a certain amount and stops

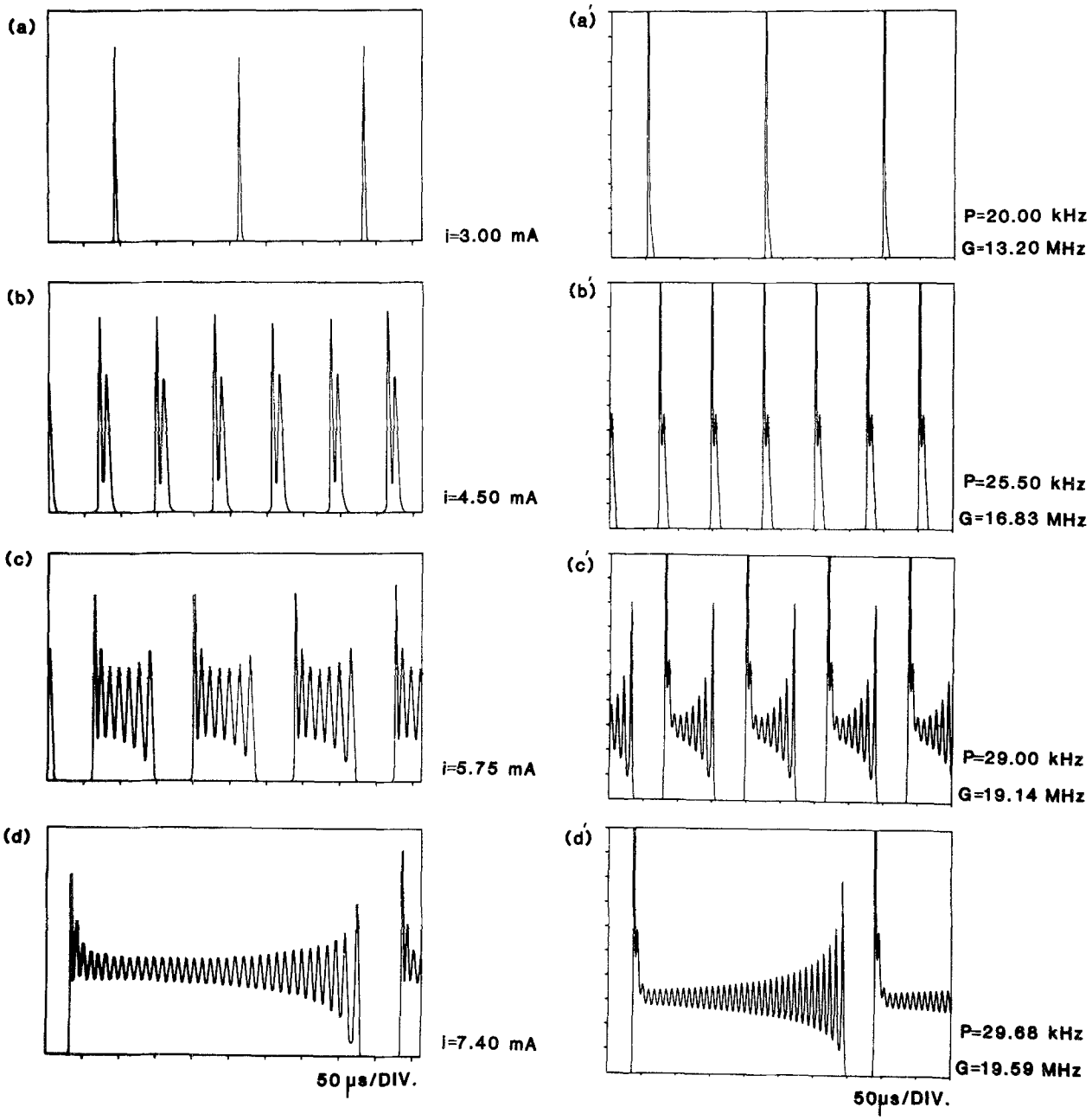

Fig. 2a–d. Observed (a–d) and calculated (a'–d') passive Q-switching pulse shapes as functions of the discharge current and the pumping rate, respectively

oscillating when the loss overcomes the gain sufficiently.

As the discharge current (the pumping rate) is increased, the pulse width becomes longer because the gain increases faster and the loss overcomes the gain later (Fig. 4). On the other hand, the recovery time between the cutoff and the onset of the laser oscillation becomes shorter because of the faster pumping. Thus the pulse period (the pulse width + the recovery time) has a minimum value as a function of the discharge current (Fig. 3).

As the He partial pressure is increased and the collisional relaxation rate of the absorbing molecules becomes faster, the loss overcomes the gain earlier and the pulse width decreases. The recovery time remains constant when the pumping rate is fixed. Therefore the pulse period decreases in the low-pressure region. In the high-pressure region where the P.Q.S. pulse has only the first spike, the P.Q.S. period is determined only by the recovery time in the laser medium and is independent of the He pressure in the absorption cell (Fig. 6).

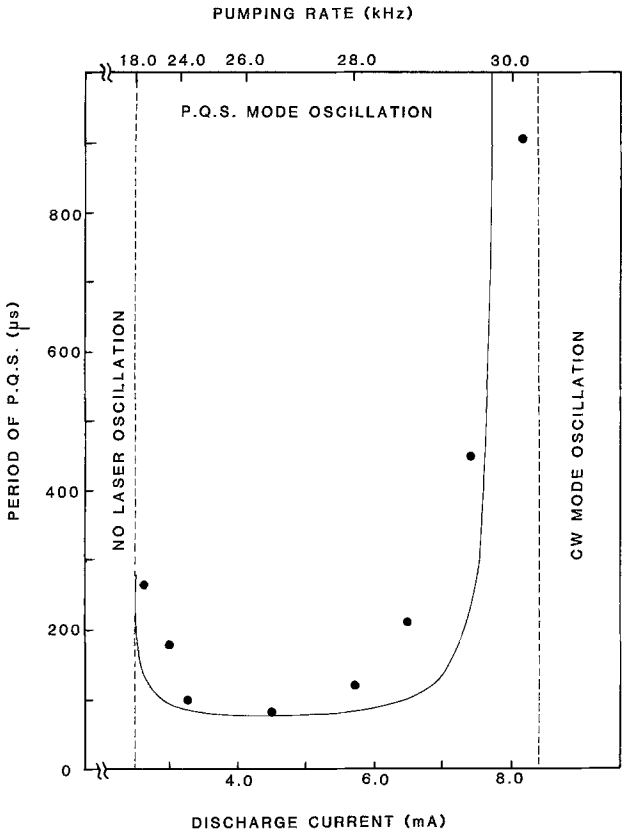

Fig. 3. Observed (represented by the dots) and calculated (represented by the solid line) dependence of the pulse period on the discharge current (the pumping rate). An empirical formula $P-P_{th}=C(i-i_{th})^{1/3}$ is used so that the calculated curve can be fitted to the observation, where $C=6.78\ \mathrm{kHz\,mA^{-1/3}}$. The dotted lines represent the boundary between no lasing mode and P.Q.S. mode and that between P.Q.S. mode and cw mode

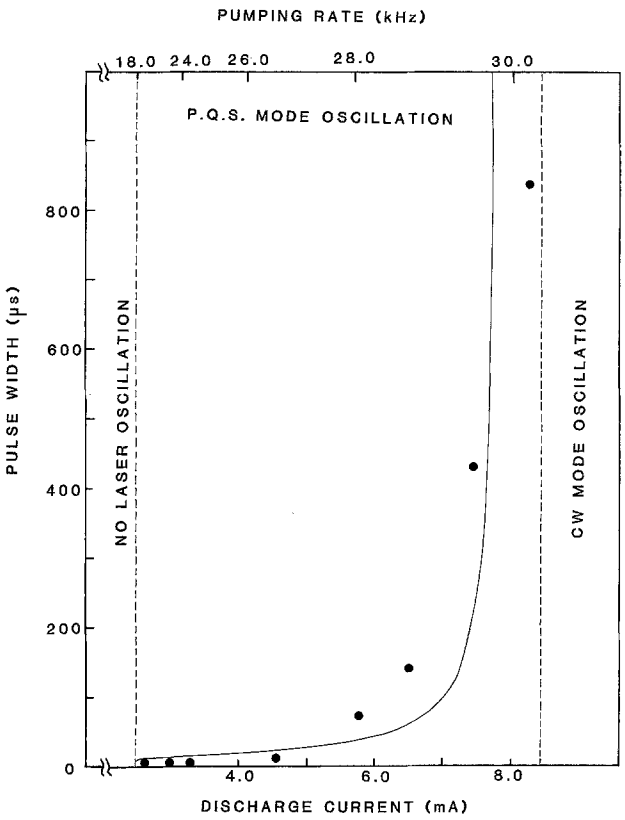

Fig. 4. Observed (represented by the dots) and calculated (represented by the solid line) dependence of the pulse width on the discharge current (the pumping rate)

The details of the pulse shape as well as the superposed undulation can not be discussed by the qualitative interpretation stated above. In the next section, it is shown that the numerical solution of the rate equations on the three-level · two-level model well reproduces the P.Q.S. pulse with the undulation.

3. Rate Equation Analysis and Discussion

A schematic diagram of the three-level · two-level model employed in the present analysis is shown in Fig. 7. The rate equations on the model are written as,

$$dn/dt=B_g n(M_1-M_2)\ l_g/L-B_a nNl_a/L+AM_1-kn\,, \quad (1)$$

$$dM_0/dt=R_{20}M_2+R_{10}M_1-(P+R_{02})M_0\,, \quad (2)$$

$$dM_1/dt=-B_g n(M_1-M_2)+PM_0+R_{21}M_2-(R_{10}+R_{12})M_1\,, \quad (3)$$

$$dM_2/dt=B_g n(M_1-M_2)+R_{12}M_1+R_{02}M_0-(R_{21}+R_{20})M_2\,, \quad (4)$$

$$dN/dt=-2B_a nN-r(N-N^*)\,, \quad (5)$$

where n is the photon density in the lasing mode, M_1 and M_2 are the population densities in the upper (0 0 1) and lower (0 2 0) laser levels, respectively. The population density in all other levels [mostly in the ground level (0 0 0)] is denoted by M_0, and N is the difference of population density between the lower level and the upper level of the absorbing molecule. The coefficients B_g and B_a are the cross sections multiplied by the light velocity c for the induced emission in the gain medium and the absorption in the absorbing medium, respectively. They are given by

$$B=\frac{2\pi\mu^2\omega}{3\varepsilon_0 h\Delta\omega}\,, \quad (6)$$

where μ is the transition dipole matrix element, ω the laser frequency, and $\Delta\omega$ the Doppler halfwidth. The length of the laser cavity, the gain tube, and the absorption cell are denoted by L, l_g, and l_a, respectively. The spontaneous emission rate of the upper laser level is represented by A, the cavity loss rate by k, and the pumping rate by P. The relaxation rate from the i level to the j level in the laser medium is written as R_{ij}, and r is the collisional relaxation rate in the absorbing gas. The thermal equilibrium value of N is denoted by N^*. The rate of spontaneous emission from

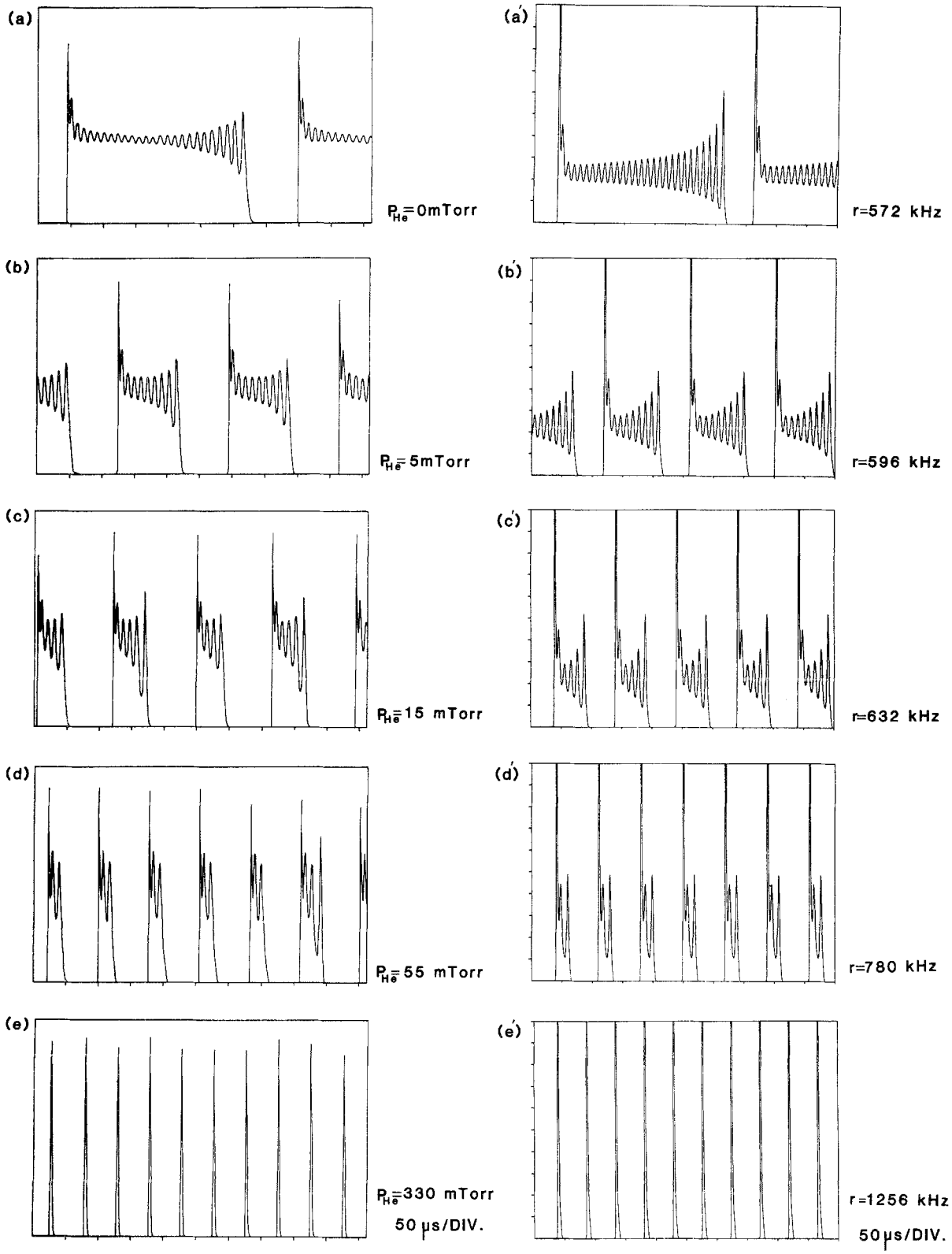

Fig. 5a–e. Observed (a–e) and calculated (a′–e′) P.Q.S. pulse shapes as functions of the He partial pressure and the relaxation rate of the absorbing gas, respectively

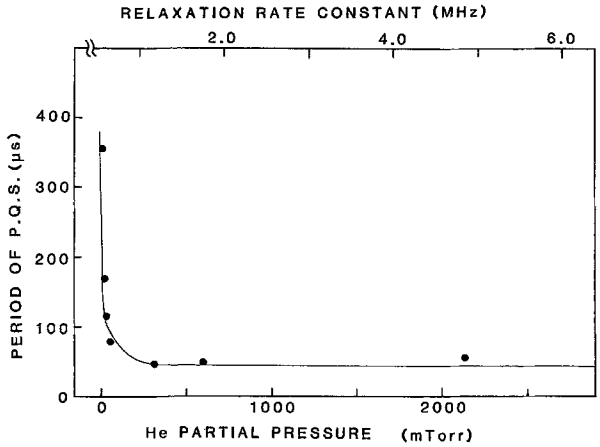

Fig. 6. Observed (represented by the dots) and calculated (represented by the solid line) dependence of the pulse period on the He partial pressure and the relaxation rate of the absorbing molecule

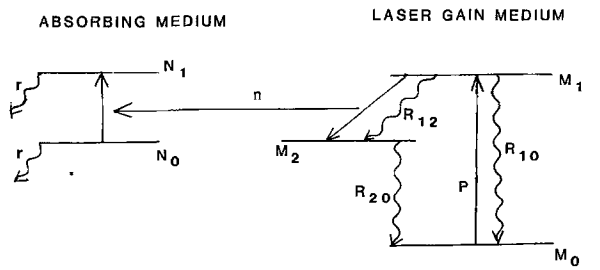

Fig. 7. Model of the gain medium and the absorbing medium employed in the rate equation analysis

Table 1. Values of the parameters used in the calculation

	In Fig. 2a′–d′	In Fig. 5a′–e′
R_{10}	6.00×10^{2} Hz	6.00×10^{2} Hz
R_{20}	4.00×10^{5} Hz	4.00×10^{5} Hz
R_{12}	1.00×10 Hz	1.00×10 Hz
P	Varied	2.50×10^{4} Hz
r	7.35×10^{5} Hz	Varied
k	2.00×10^{6} Hz	2.00×10^{6} Hz
$B_gM_1^*l_g/L(\equiv G)$	Varied	1.65×10^{7} Hz
$B_aN^*l_a/L$	1.03×10^{7} Hz	8.00×10^{6} Hz
B_a/B_g	36.0	36.0

the upper laser level in (3) and (4), and that from the upper absorber level in (1) and (5) are neglected.

The set of the rate equations is numerically integrated by the Euler method. One step of integration is 1 ns and short enough compared with the time constants involved in the equations.

The calculated pulse shapes are shown in Fig. 2a′–d′ together with the corresponding observed pulses (a–d) for several values of the discharge current. Agreements in apparent pulse shapes between observation and calculation are very good. The calculation well reproduces even detailed behaviour of the undulation on

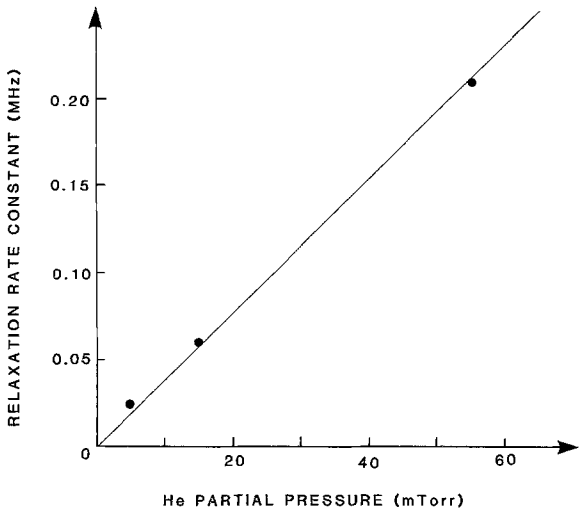

Fig. 8. Relation between the He partial pressure and the collisional relaxation rate against He obtained from the correspondences between the observed and calculated pulse shapes in Fig. 5

the P.Q.S. pulse. The period is well defined in the middle part of the pulse where the undulation amplitude stays constant, while the period of undulation becomes longer at the end of the pulse tail (Fig. 2d and d′). The calculation is carried out using different sets of P and $B_gM_1^*l_g/L(\equiv G)$ parameters shown in the figure, where M_1^* is the equilibrium value of M_1 in the absence of the laser radiation. The value of M_1^* is assumed to be proportional to P. Other parameters are fixed to the values in Table 1.

The observed dependence of the period of pulses and the pulse width on the discharge current as well as the calculated dependence (solid line) on the pumping rate is shown in Figs. 3 and 4, respectively. The relation of the pumping rate P to the discharge current i is not well known. However the calculated curves can be fitted to the observation fairly well if an empirical formula,

$$P-P_{\mathrm{th}}=C(i-i_{\mathrm{th}})^{1/3} \tag{7}$$

is introduced, where P_{th} and i_{th} are the threshold values and $C=6.78\,\mathrm{kHz\ mA^{-1/3}}$.

The pulse shapes calculated as a function of the relaxation rate constant r are shown in Fig. 5a′–e′. The calculation very well reproduces the observed pulse shapes with the undulation. The relaxation rates used in the calculation are shown in the figure, and other fixed parameters appear in Table 1. As shown in Fig. 6, a good agreement between the calculation (solid line) and the observation is obtained for the dependence of the pulse period on the partial pressure of He. The relation between the partial pressure of He and the collisional relaxation rate against He is obtained from the correspondences between the calculated and observed pulse shapes, and shown in Fig. 8. The colli-

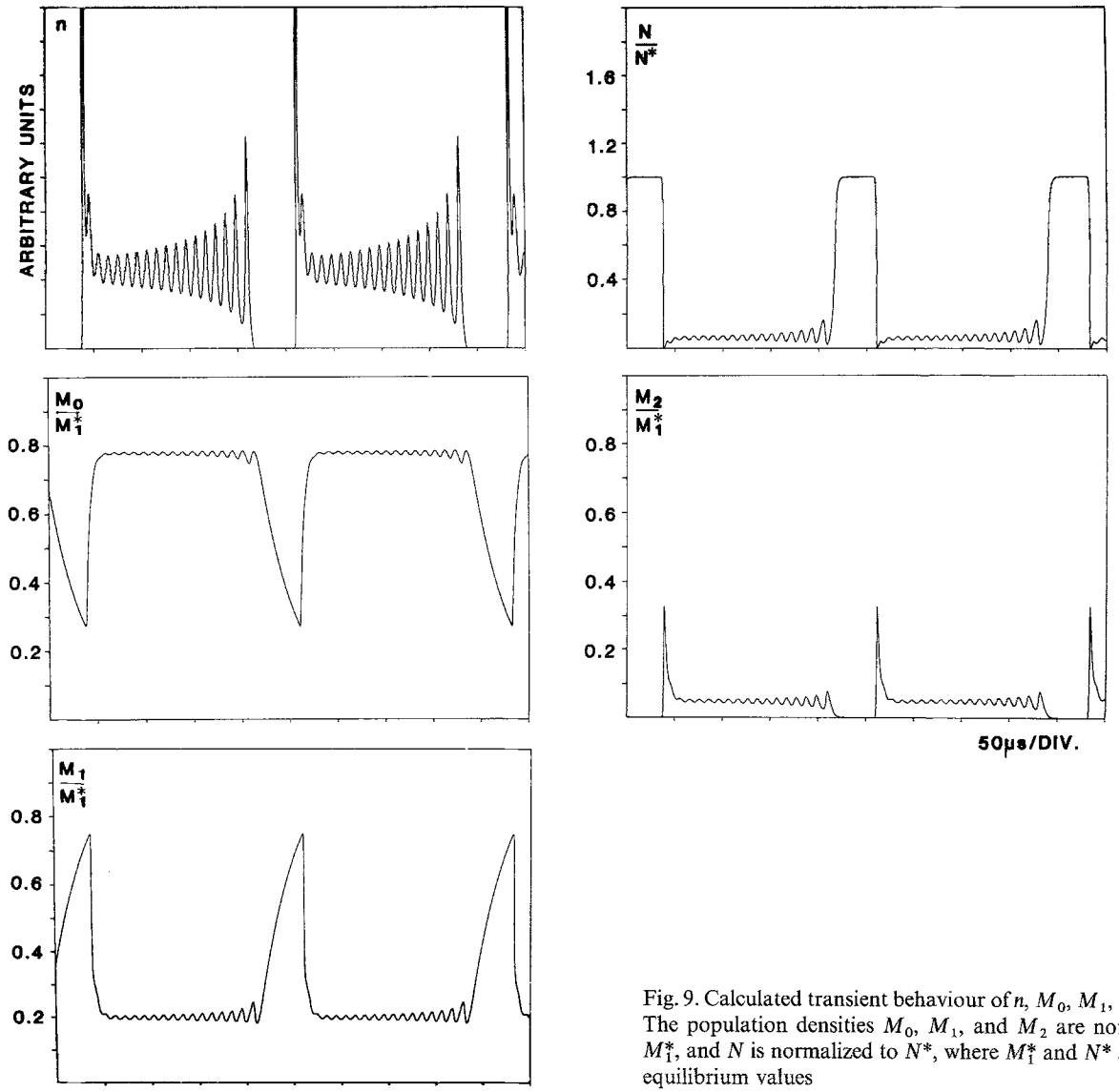

Fig. 9. Calculated transient behaviour of n, M_0, M_1, M_2, and N. The population densities M_0, M_1, and M_2 are normalized to M_1^*, and N is normalized to N^*, where M_1^* and N^* are thermal equilibrium values

sional relaxation rate constant of HCOOH against He (foreign gas broadening parameter) is determined to be 3.8 MHz $Torr^{-1}$.

Cheo reported that the rate of excitation transfer from N_2 ($v=1$) to CO_2 (0 0 1) was 1.9×10^4 $Torr^{-1}\,s^{-1}$, $R_{100-000}=385$ $Torr^{-1}\,s^{-1}$ (against CO_2), $R_{020-010}=4.7\times10^3$ $Torr^{-1}\,s^{-1}$ (against He), and the fluorescence rate from the (0 0 1) level was 350 Hz [22]. Using these rate constants, the values of parameters to be used in the present analysis are calculated to be $P=15$ kHz (if most of N_2 are excited to the $v=1$ level), $R_{10}=0.66$ kHz, and $R_{20}=30$ kHz. The values of P and R_{10} reasonably agree with those in Table 1, however R_{20} shows a large discrepancy. Cheo assumed that the (0 2^0 0) and the (1 0^0 0) levels decayed with the same relaxation rate because they were mixed by the Fermi resonance. However, DeTemple et al. reported the different decay constants in the observation of the pulsed oscillation between the 9.6 μm laser and the 10.6 μm laser [23]. Recently Ueda and Shimizu (F.O.) reported that the relaxation rate from the lower level of the 9.6 μm laser was much faster than that of the 10.6 μm laser which corresponded to the value proposed by Cheo [19]. The value of R_{20} used in the present calculation is consistent with the idea of detailed discussion of the process. The value of R_{12} is estimated from R_{10} comparing the calculated Z-number of the (0 0^0 1)–(0 2^0 0) process with that of the relaxation processes from the (0 0^0 1) level to all other levels [22]. The relaxation rates R_{21} and R_{02} are negligibly small and fixed to 0. The collisional relaxation rate constant of HCOOH is assumed to be 9.5 MHz $Torr^{-1}$. This value reasonably agrees with the results of Minowa et al. [24]. The cavity loss rate k is estimated from reflectance of the mirror and the grating. The value of $B_aN^*l_a/L$ is calculated assuming

that the transition dipole matrix element of the absorptive line is 0.1 D. The values of the linear gain rate $B_g M_1^* l_g/L(\equiv G)$ which appear in Fig. 2a′–d′ and the second column of Table 1 (13.2 ~ 19.6 MHz) are reasonable compared with the sum of the linear absorption loss rate $B_a N^* l_a/L$ (10.3 or 8.0 MHz) and the cavity loss rate (2.0 MHz). The ratio B_a/B_g is evaluated assuming that the transition dipole matrix element of the relevant transition of CO_2 is 0.017 D.

The relaxation oscillation in the output of the 10.6 μm laser observed by Ueda and Shimizu (F.O.) is caused in the balance between the induced emission and the relaxation of the lower laser level [19]. The relaxation of the lower level increases the population inversion. Therefore, it plays the same role as pumping. They could not observe the relaxation oscillation in the 9.6 μm laser because the relaxation rate was so fast that the laser oscillation terminated in a single pulse. However if the cw pumping is present, it can take place also in the 9.6 μm laser. Shimoda reported that the output of the ruby laser showed the undamped relaxation oscillation due to the saturable absorber in the laser medium [20]. The absorption coefficient is large for the weak electric field and small for the strong electric field in a saturable absorber. Thus a saturable absorber within a laser cavity can amplify the variation of the laser intensity.

Figure 9 shows the transient behavior of n, M_0, M_1, M_2 and N in calculation. The lower laser level plays an important role to produce the undulation. We propose the mechanism of the undamped undulation on the P.Q.S. pulse tail as follows. The undulation is the relaxation oscillation caused in the balance between the induced emission from the upper laser level and the relaxation of the lower laser level. The amplitude of the undulation is undamped or even amplified because of the presence of the saturation effect in the absorption loss. Arimondo et al. observed the transient relaxation oscillation in the cw mode right after the loss modulation by a Stark pulse [14, 15]. They claimed that the relaxation oscillation turned into the P.Q.S. pulse when the excitation was reduced. The period of the relaxation oscillation smoothly extended into that of the P.Q.S. pulse [14, 15, 17]. That relaxation oscillation obviously occurred in the balance between the pumping and the induced emission. On the other hand the relaxation oscillation in the present experiment is observed being superposed on the P.Q.S. pulse and caused by the relaxation of the lower laser level.

4. Summary

The clear-cut signals of the P.Q.S. pulse with the undamped undulation observed in the output of a CO_2 9.6 μm laser using HCOOH as a saturable absorber have allowed us to analyze the characteristics of the transient laser oscillation quantitatively. It is found that the simple model of the laser system (Fig. 7) is good enough to explain the complicated transient behavior of the laser pulse. The numerical solution of the rate equations very well reproduces the detailed structures of the pulse shape with the undulation and the dependence of the pulse period and the pulse width on laser parameters. The mechanism of the undamped undulation has been understood as the relaxation oscillation caused in the balance between the induced emission and the relaxation of the lower laser level. The collisional relaxation rate constant of HCOOH against He is also determined.

Acknowledgements. The authors gratefully acknowledge Mr. Odashima for his help in the experiment, Dr. Matsushima for helpful advices and Mr. Onae, Miss Matsuo, Prof. F.O. Shimizu, and Prof. E. Arimondo for discussions.
This work was supported by a Grant-in Aid for Special Project Research from the Ministry of Education, Science, and Culture.

References

1. O.R. Wood, S.E. Schwarz: Appl. Phys. Lett **11**, 88–89 (1967)
2. P.L. Hanst, J.A. Morreal, W.J. Henson: Appl. Phys. Lett. **12**, 58–61 (1968)
3. J.T. Yardley: Appl. Phys. Lett. **12**, 120–122 (1968)
4. N.V. Karlov, G.P. Kuz'min, Yu. Petrov, A.M. Prokhorov: JETP Lett. **7**, 134–136 (1968)
5. W.F. Krupke: Appl. Phys. Lett. **14**, 221–222 (1969)
6. T.Y. Chang, C.H. Wang, P.K. Cheo: Appl. Phys. Lett. **15**, 157–159 (1969)
7. S. Marcus: Appl. Phys. Lett. **15**, 217–219 (1969)
8. R.E. Jensen, M.S. Tobin: IEEE J. QE-**6**, 477–478 (1970)
9. I. Burak, P.L. Houston, D.G. Sutton, J.I. Steinfeld: IEEE J. QE-**7**, 73–82 (1971)
10. J.J. Wynne, F. Shimizu: IEEE J. QE-**8**, 676–677 (1972)
11. J. Dupré, F. Meyer, C. Meyer: Rev. Phys. Appl. (Paris) **10**, 285–293 (1975)
12. F. Meyer, J. Dupré, C. Meyer: Can. J. Phys. **54**, 205–210 (1976)
13. W. Kreiner: IEEE J. QE-**17**, 16–20 (1976)
14. E. Arimondo, P. Glorieux: Appl. Phys. Lett. **33**, 49–51 (1978)
15. E. Arimondo, F. Casagrande, L.A. Lugiato, P. Glorieux: Appl. Phys. B**30**, 57–77 (1983)
16. J. Heppner, Z. Šolajić, G. Merkle: Appl. Phys. B**35**, 77–82 (1984)
17. E. Arimondo, E. Menchi: Appl. Phys. B**37**, 55–61 (1985)
18. Z. Šolajić, J. Heppner: Appl. Phys. B**33**, 23–27 (1984)
19. K. Ueda, F.O. Shimizu: Jpn. J. Appl. Phys. **23**, 1038–1044 (1984)
20. K. Shimoda: In Proc. Symp. on Optical Masers, Polytechnic Institute of Brooklyn (1963) pp. 95–108
21. B.M. Landsberg, D. Crocker, R.J. Butcher: J. Mol. Spectrosc. **92**, 67–76 (1982)
22. P.K. Cheo: *Lasers 3* (Dekker, New York 1971) pp. 111–267
23. T.A. DeTemple, D.R. Suhre, P.D. Coleman: Appl. Phys. Lett. **22**, 349–350 (1973)
24. T. Minowa, Y. Matsuo, H. Kuze, T. Shimizu: J. Chem. Phys. **78**, 1861–1866 (1983)